High-SNR ultrasound-modulated optical tomography with intense acoustic bursts

Chul hong Kim, Roger J. Zemp, Lihong V. Wang

Chul hong Kim, Roger J. Zemp, Lihong V. Wang, "High-SNR ultrasound-modulated optical tomography with intense acoustic bursts," Proc. SPIE 6086, Photons Plus Ultrasound: Imaging and Sensing 2006: The Seventh Conference on Biomedical Thermoacoustics, Optoacoustics, and Acousto-optics, 608617 (6 March 2006); doi: 10.1117/12.648533

Event: SPIE BiOS, 2006, San Jose, California, United States

High-SNR Ultrasound-Modulated Optical Tomography with Intense Acoustic Bursts

Chul hong Kim, Roger J. Zemp, and Lihong V. Wang*

Optical Imaging Laboratory, Department of Biomedical Engineering, 3120 TAMU,
Texas A&M University, College Station, Texas 77843-3120

ABSTRACT

We present a novel signal-enhancement method for ultrasound modulated optical tomography that can increase the amount of modulated light, compared to previous methods. By applying intense acoustic bursts, particle displacements of several microns are possible at a very local scale. A CCD camera captured the speckle pattern emerging from a laser-illuminated tissue phantom and differences in laser speckle contrast were measured between ultrasound on and off states. When CCD triggering was synchronized with burst initiation, ultrasound radiation force-induced displacements were detected with our technique, and resulting shear waves were shown to degrade image contrast and spatial resolution. Deleterious effects of shear waves were minimized by delaying CCD camera acquisition several ms until shear waves are adequately attenuated. Our system signal-to-noise ratio (SNR) is sufficiently high to perform UOT scanning without signal averaging. Because of substantially improved SNR compared to previous techniques, the use of intense acoustic burst is a new promising method for ultrasound modulated optical tomography.

Keywords: Ultrasound modulated optical tomography, speckle-contrast detection, acoustic radiation force, shear waves.

INTRODUCTION

1. Motivation

Ultrasound modulated optical tomography[1,2] (UOT) is a novel bio-photonic imaging technique which takes advantage of strong optical contrast and high ultrasonic spatial resolution. The principle of UOT is that a high coherent laser illuminates a light-scattering sample, while being insonified with ultrasound. Light passing through the ultrasonic sample volume is acoustically modulated from time-varying particle displacements and changes in refractive index such that each optical speckle spot has a time-varying modulation component due to the ultrasonic interaction.[3-5] By observing the modulated component of light at each ultrasonic sample volume position, images may represent the optical properties of the tissue. A major challenge in UOT is the low signal-to-noise ratio because of both low modulation depth and uncorrelated speckle grains. In order to detect weak modulated signals effectively, a number of groups have devoted efforts to develop new detection methods, including parallel detection with CCD cameras[6-8], Fabry-Perot interferometer[9], and photo-refractive crystal techniques[10], to overcome this problem. In this paper, using a speckle-contrast detection technique[11], we explored the use of intense ultrasound bursts, instead of the use of continuous-wave or pulsed ultrasound.[12] By reducing the duty cycle on the ultrasonic transducer, it is possible to use much higher pressures, thus improving the ultrasound-modulated light signal level. Additionally, during timescales on the order of a ms, intense acoustic bursts induce localized tissue displacement due to acoustic radiation force. We experimentally demonstrate slight but statistically significant radiation-force-enhancement of UOT signals beyond pure ultrasound mechanisms. This enhancement, however, comes with a cost. Shear waves due to ultrasound radiation force are shown to degrade UOT image contrast and spatial resolution, however, this transient effect is mitigated as transient shear-displacements propagate away from the pushing region and are attenuated. By triggering CCD camera image acquisition several ms after the acoustic burst generation, pure ultrasound mechanisms dominate over shear-wave transients. We compare signal levels with three mechanisms; the continuous-wave ultrasound mechanism with low pressure, the transient effect during the pushing phase of an ultrasonic burst, and the steady-state effect during the

* lwang@tamu.edu; phone +1 979 847 9040; fax +1 979 845 4450

Photons Plus Ultrasound: Imaging and Sensing 2006: The 7th Conference on Biomedical Thermoacoustics, Optoacoustics, and Acousto-optics, edited by A. A. Oraevsky, et. al
Proc. of SPIE Vol. 6086, 608617 (2006) • 1605-7422/06/$15 • doi: 10.1117/12.648533

oscillating phase of an ultrasonic burst. To demonstrate the SNR advantage of our method, we show high contrast UOT images of phantoms without signal averaging, an important step towards moving UOT towards *in vivo* imaging studies.

2. Theory

Acoustic radiation force (ARF) is generated when ultrasound interacts with an interface of mismatched acoustic impedance, or interacts with ultrasonic absorbers.[13] When this occurs there is an inherent momentum transfer which generates a force. Under an acoustic plane wave assumption, ultrasound radiation force has the form:

$$F = W / c \quad (1)$$

where, for a focused ultrasonic wave, F is the ARF at the focal spot, W is the absorbed ultrasonic beam power at the focal spot, and c is the speed of sound in the medium. These effects have been used in various imaging techniques to elucidate mechanical properties of tissue. Nightingale *et al.*[14] used transient radiation force to perform Acoustic Radiation Force Impulse Imaging, wherein acoustic radiation force displaced tissue and the resulting motion was tracked with speckle-tracking methods. Greenleaf *et al.*[15] performed imaging by using the beat-frequency of two con-focal narrow band acoustic fields to generate local radiation-force that induced tissue-dependent acoustic waves detected by sensitive hydrophones.

EXPERIMENTS

The experimental setup is shown in Figure 1 with a Cartesian coordinate system as a reference. The light source (Coherent, Verdi; 532 nm wavelength) illuminated a tissue mimicking sample. The average laser power delivered to the phantom during CCD exposure period was ~12mW/cm^2, a value below present safety limits. A focused ultrasound transducer (Ultran, VHP100-1-138; 1 MHz central frequency, 25.4 mm lens diameter, 38 mm focal length) generated acoustic waves. The focal zone of an ultrasonic wave was ~2 mm in width and ~20 mm in length. The ultrasound peak pressure at the focal spot for image experiments was applied up to 1.5 MPa, so the Mechanical Index (MI) at this frequency was ~1.5, which is below 1.9, the present maximum permissible MI for diagnostic ultrasound systems.[16] We used a gelatin-cornstarch (10%-wt gelatin and 10%-wt cornstarch) phantom with reduced scattering coefficient of ~9.2 cm^{-1} as measured by an Oblique-Incidence Reflectometer.[17] The light transmitted through the sample yielded a speckle pattern which was detected by a digital CCD camera (Basler, A312f; 12-bit, 640×480 pixels). A function generator (Agilent, 33250A) synthesized 2-20 ms bursts that were subsequently amplified by an RF amplifier (ENI, Inc., 325LA) to drive the ultrasound transducer. Burst initiation triggered a pulse-delay generator (Stanford Research, DG535) that produced two CCD trigger pulses for each burst. A low 1-Hz duty cycle was used to prevent damage to the transducer. One burst-synchronized frame was captured on the CCD camera, after which an image was taken with no ultrasound. We measured laser speckle contrast on the CCD surface with and without the ultrasound modulation every second. CCD image capture can either be done at the initiation of an 8 ms burst (to see transient acoustic radiation force (TARF) effect) or near the end of a long burst, where transient effects have adequately attenuated (we refer to this as quasi continuous wave (quasi-CW) ultrasound). The exposure time of the CCD camera was set to 2 ms. We define our signal as the difference between ultrasound ON and OFF in speckle contrast measurements.

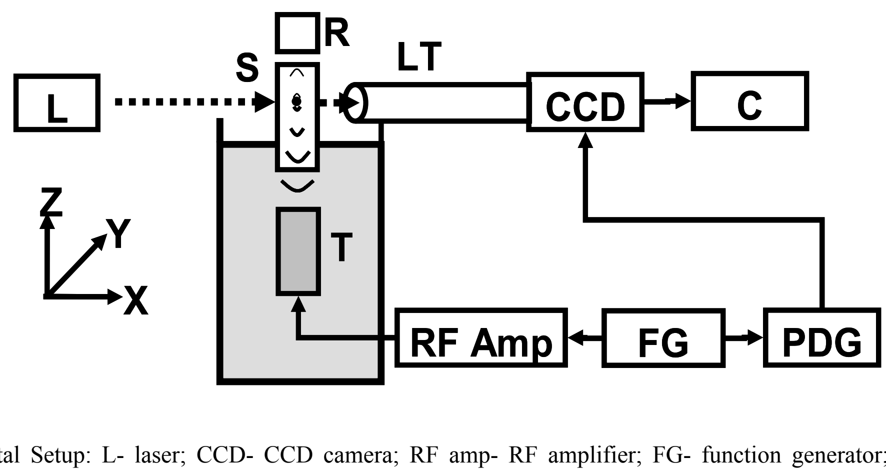

Figure 1: Experimental Setup: L- laser; CCD- CCD camera; RF amp- RF amplifier; FG- function generator; PDG- pulse-delay generator; T- ultrasound transducer; S- sample; LT- lens tube; R- rubber; C-personal computer.

RESULTS AND DISCUSSIONS

1. Signal enhancement due to intense acoustic bursts and shear wave effects

To show signal enhancement using intense acoustic bursts, we measured the signal with increasing ultrasonic pressure (Figure 2a). As the pressure increases, the signal becomes larger and the difference between the TARF and quasi-CW regime becomes larger. The signal starts saturating after the ultrasonic pressure goes higher than ~2MPa. The SNR, defined as the mean of change in speckle contrast divided by the root-mean-square standard deviations of ultrasound on and off, with 1.5MPa quasi-CW was 260 compared to 287 with 1.5MPa TARF and 32 with 0.3MPa CW (Figure 2a). The SNR enhancement of quasi-CW mechanism over CW mechanism is about 8 times larger, but the SNR enhancement of TARF mechanism over quasi-CW mechanism is only 10% larger. Quasi-CW method can provide the comparable SNR to TARF method but is not affected by shear wave displacement and propagation. In addition, comparison of signals with different CCD trigger delay times can distinguish the effects of TARF and quasi-CW (Figure 2b). To show this, we applied a 20 ms, ultrasonic burst of ~2 MPa peak pressure, and triggered the CCD camera at 0, 2, 4, ···, 18 ms delays following the burst initiation. The largest change in speckle contrast is generated, when the burst and CCD trigger are synchronized (with zero delay). After this point, the TARF effect attenuates and the signal decreases as it approaches a steady-state condition, where quasi-CW ultrasound mechanisms dominate TARF mechanisms (Figure 2b). Although TARF offers signal enhancement over quasi-CW methods for the same acoustic pressure, the relative enhancement is only about 10% at the ultrasonic pressure of 2 MPa.

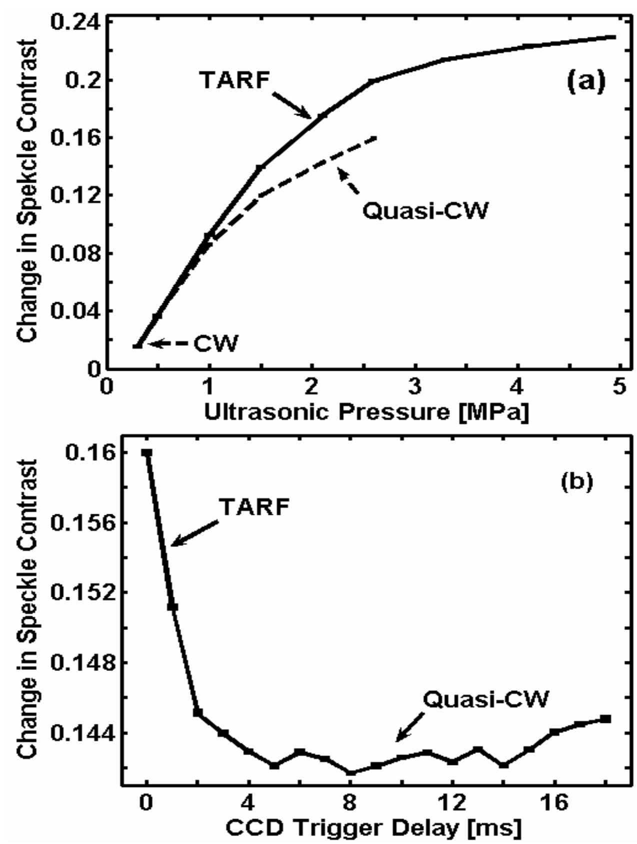

Figure 2: (a) Comparison of signals applying TARF and quasi-CW at different ultrasonic pressures. (b) Comparison of signals in TARF and quasi-CW regimes varying CCD trigger delay times with the ultrasonic pressure of 2 MPa.

2. 1D images

To investigate the potential of using intense acoustic bursts for optical imaging, we scanned phantoms and compared image contrast and spatial resolution of images acquired during the TARF and quasi-CW regimes to images formed using lower pressure CW ultrasound. We imaged a gelatin-cornstarch phantom with two Trypan-Blue dyed objects (2.1 mm × 2.1 mm × 10 mm and 2.1 mm × 1.8 mm × 10 mm) separated by 8 mm from center-to-center. As the ultrasonic pressure increases, the signal likewise increases. In addition, two absorbing objects are clearly seen in Figure 3. At the same pressure, the signal with TARF mechanism is only 10% larger than the signal with quasi-CW. This increase in signal comes with higher *absolute* image contrast and without significant loss in spatial resolution. The *absolute* image contrasts with TARF and quasi-CW are five times greater than the one with CW. Spatial resolution defined as the one-way distance between the 25% and 75% of the maximum is approximately 2.2 mm in all of three mechanisms, which is comparable to the ultrasonic beam waist.

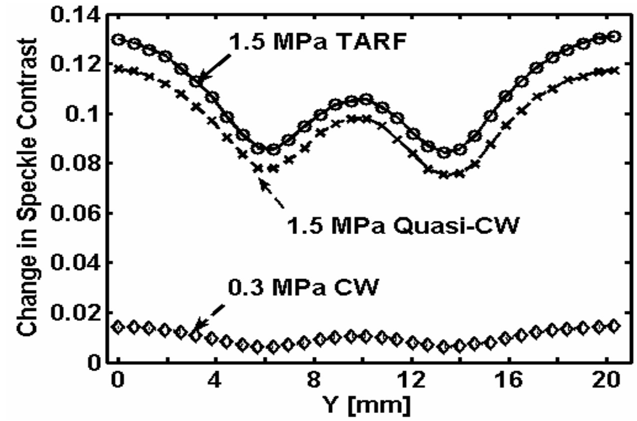

Figure 3: Comparison of 1D images of two Trypan-blue dyed objects in a 1.9-cm thick tissue mimicking phantom with varying ultrasonic pressures.

3. Image degradation due to shear waves

To investigate shear wave effects on UOT images, we applied higher pressures up to 1.9 MPa using both TARF and quasi-CW mechanisms. Higher pressures generate larger force and larger shear displacement. In addition, TARF mechanism is affected by shear wave propagation. Increasing pressure increases the amount of non-local shear-wave induced modulation (Figure 4a). Increasing CCD exposure time also degrades image quality because shear wave propagation endangers non-locality of light modulation. 1D images using 2, 4, and 5 ms CCD exposure time CCD exposure times are shown in the Figure 4b. It is clear that the two objects, represented as dips in the signal, are most distinct for the shortest CCD exposure time.

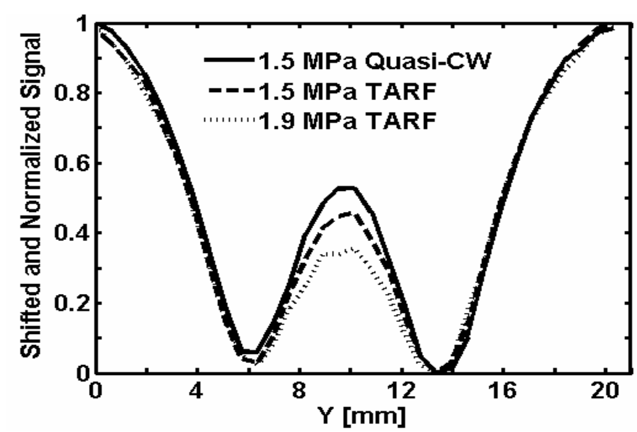

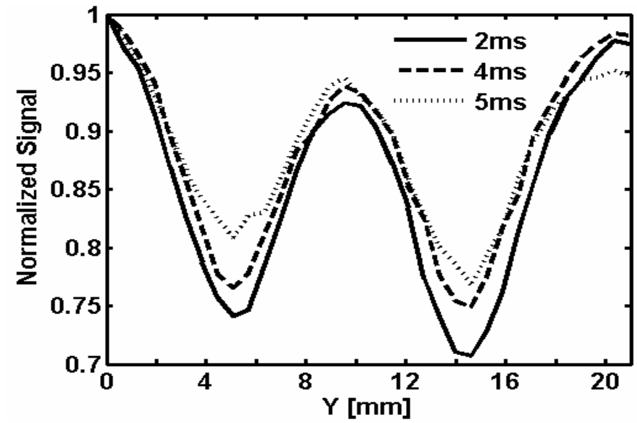

Figure 4: Image degradation as a function of (a) increasing ultrasonic pressure and (b) extending CCD exposure time.

4. 2D images

4.1. 2D imaging using the TARF mechanism

Figure 5 shows a 2D image obtained using 1.5 MPa, and synchronizing the 2 ms burst and CCD triggering to allow sensitivity to the transient acoustic radiation force mechanism. 8 measurements were averaged. The gelatin-cornstarch sample with 19 mm thickness contained two Trypan-Blue dyed objects (separated by 11 mm, from center to center). The sizes of the two objects were approximately 2.1 mm × 2.4 mm × 13 mm and 1.4 mm × 2.5 mm × 13 mm along the *X*, *Y*, and *Z* axes. In the image, the objects are clearly seen with a relative image contrast of 36% and a resolution of ~2.3 mm.

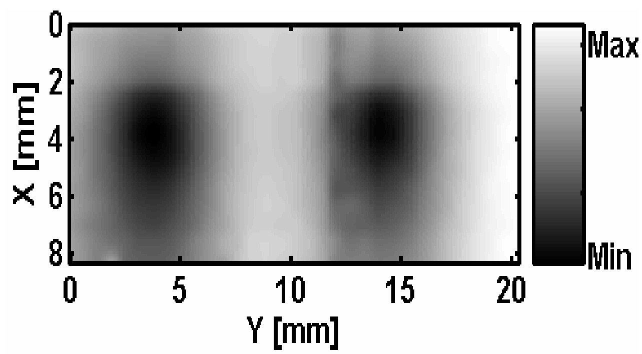

Figure 5: Two-dimensional image of two Trypan-Blue dyed objects embedded in a 1.9 cm-thick tissue mimicking phantom acquired using TARF.

4.2. 2D images using quasi-CW mechanism

Like the TARF mechanism, the quasi-CW method can also provide substantial SNR for 2D imaging. As in section 4.1 we scanned the 1.9 mm thick phantom possessing two Trypan-blue dyed targets. The sizes of the two objects were approximately 2.0 mm × 2.0 mm × 12.3 mm and 2.0 mm × 1.3 mm × 12.3 mm along the *X*, *Y*, and *Z* axes. An ultrasonic pressure of 1.5 MPa was applied. The CCD exposure time was set to 2 ms. Only 1 pair of on-off measurements were taken for each image pixel. We performed no averaging. In Figure 6, the objects are clearly seen with a *relative* image contrast of 31% and a resolution of ~2.0 mm.

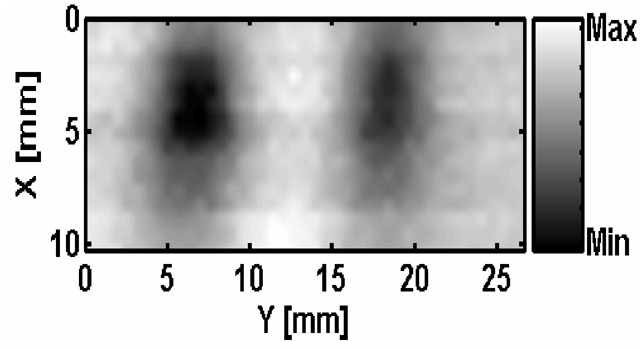

Figure 6: Two-dimensional image of two Trypan-Blue dyed objects embedded in a 1.9 cm-thick tissue mimicking phantom acquired using quasi-CW.

CONCLUSIONS

In summary, this research has demonstrated that intense acoustic bursts can provide statistically significant UOT signal enhancement, higher *absolute* image contrast and comparable spatial resolution compared to continuous-wave mechanism with low pressure. Because of the benefits of higher SNR, the scanning time may be reduced by one or two orders of magnitude to get an image. Furthermore, the imaging system was extremely robust to environmental disturbances. Imaging without the need for averaging is a crucial step forward for research in UOT, a field previously hindered by extraordinarily weak signals. This work shows progress in this direction. Future work may combine this technique with other UOT detection techniques such as parallel detection with CCD cameras, Fabry-Perot interferometery, and photo-refractive crystal techniques.

ACKNOWLEDGEMENT

We thank X. Xiao, S. Sakadžic´ for fruitful scientific discussions and A. Garcia-Uribe for assistance with optical property measurements. This research was supported by the National Institutes of Health grant CA094267. L. Wang's e-mail address is lwang@tamu.edu.

.

REFERENCES

1. F. A. Marks, H. W. Tomlinson, and G. W. Brooksby, "Comprehensive approach to breast cancer detection using light: photon localization by ultrasonic modulation and tissue characterization by spectral discrimination," in Photon Migration and Imaging in Random Media and Tissue, B. Chance and R. R. Alfano, eds., Proc. SPIE 1888, pp. 500–510 (1993).
2. L.-H. Wang, S. L. Jacques, and X. Zhao, "Continuous-wave ultrasonic modulation of scattered laser light to image objects in turbid media," Opt. Lett. 20, pp. 629–631 (1995).
3. W. Leutz and G. Maret, "Ultrasonic modulation of multiply scattered light," Phys. B 204, pp. 14–19 (1995).
4. L.-H. V. Wang, "Mechanisms of ultrasonic modulation of multiply scattered coherent light: an analytic model," Phys. Rev. Lett. 87, (043093) pp. 1–4 (2001).
5. S. Sakadzˇic´ and L.-H. V. Wang, "Ultrasonic modulation of multiply scattered coherent light: an analytical model for anisotropically scattering media," Phys. Rev. E 66, (026603) pp. 1–9 (2002).
6. S. Leveque, A. C. Boccara, M. Lebec, and H. Saint-Jalmes, "Ultrasonic tagging of photon paths in scattering media: parallel speckle modulation processing," Opt. Lett. 24, pp. 181–183 (1999).
7. G. Yao, S. Jiao, and L.-H. Wang, "Frequency-swept ultrasound-modulated optical tomography in biological tissue by use of parallel detection," Opt. Lett. 25, pp. 734–736 (2000).
8. M. Gross, P. Goy and M. Al-Koussa, "Shot-noise detection of ultrasound-tagged photons in ultrasound-modulated optical imaging," Opt. Lett. 28, pp. 2482-2484 (2003).
9. S. Sakadžic´ and L.-H. V. Wang, "High-resolution ultrasound-modulated optical tomography in biological tissues," Opt. Lett. 29, pp. 2770-2772 (2004).

10. T. W. Murray, L. Sui, G. Maguluri, R. A. Roy, A. Nieva, F. Blonigen, C. A. DiMarzio, "Detection of ultrasound-modulated photons in diffuse media using the photorefractive effect," Opt. Lett. 29, pp. 2509-2511 (2004).
11. J. Li, G. Ku, and L.-H. V. Wang, "Ultrasound-modulated optical tomography of biological tissue using contrast of laser speckles," Appl. Opt. 41, pp. 6030–6035 (2002).
12. A. Lev and B. G. Sfez, "Pulsed ultrasound-modulated light tomography," Opt. Lett. 28, pp. 1549-1551 (2003).
13. G. R. Torr, "The acoustic radiation force," Am. J. Phys. 52, pp. 402-408 (1984).
14. K. Nightingale, M. S. Soo, R. Nightingale, and G. Trahey, "Acoustic radiation force impulse imaging: *in vivo* demonstration of clinical feasibility," Ultra. Med. Biol. **28**, pp. 227-235 (2002).
15. M. Fatemi and J. F. Greenleaf, "Ultrasound-stimulated vibro-acoustic spectrography," Science, **280**, pp. 82-85 (1998).
16. Diane Dalecki, "Mechanical bioeffects of ultrasound," Annu. Rev. Biomed. Eng.. **6**, pp. 18.1-18.20 (2004).
17. G. Marquez and L.-H. Wang, "White light oblique incidence reflectometer for measuring absorption and reduced scattering spectra of tissue-like turbid media," Opt. Express. **1,** pp. 454–460 (1997).